Table S1. The thermodynamic cycle used to calculate the enthalpy of drop solution (ΔH_{ds}) of Pr_2O_3 in $3Na_2O{\cdot}4MoO_3$ at 800 °C.

reaction	ΔH (kJ mol^{-1})
$PrPO_4$ (s, 25 °C) → $1/2Pr_2O_3$ (soln, 700 °C) + $1/2P_2O_5$ (soln, 700 °C)	$\Delta H_1 = 147.54 \pm 0.96$ [1]
Pr_2O_3 (s, 25 °C) → Pr_2O_3 (soln, 700 °C)	ΔH_2
P_2O_5 (s, 25 °C) → P_2O_5 (soln, 700 °C)	$\Delta H_3 = -164.60 \pm 0.85$ [2]
$1/2Pr_2O_3$ (s, 25 °C) + $1/2P_2O_5$ (s, 25 °C) → $PrPO_4$ (s, 25 °C)	$\Delta H_4 = -326.11 \pm 8.13$ [1]
$\Delta H_2 = 2\Delta H_1 - \Delta H_3 + 2\Delta H_4 = -192.54 \pm 16.40$ kJ mol^{-1}	
Pr_2O_3 (s, 700 °C) → Pr_2O_3 (s, 800 °C)	$\Delta H_5 = 14.69 \pm 0.22$ [3]
Pr_2O_3 (s, 25 °C) → Pr_2O_3 (soln, 800 °C)	ΔH_{ds}
$\Delta H_{ds} = \Delta H_2 + \Delta H_5 = -177.85 \pm 16.40$ kJ mol^{-1}	

Table S2. Born–Haber cycles used to calculate the lattice energies (U) of BLnC and BGLC samples.

reaction	ΔH (kJ mol^{-1})
Ba (s, 25 °C) → Ba (g, 25 °C)	$\Delta H_1 = 179.8 \pm 5.0$ [4]
Ba (g, 25 °C) → Ba^{2+} (g, 25 °C) + $2e^-$	$\Delta H_2 = 1468.071 \pm 0.001$ [5]
Ln (s, 25 °C) → Ln (g, 25 °C)	ΔH_3
Ln (g, 25 °C) → Ln^{3+} (g, 25 °C) + $3e^-$	ΔH_4
Co (s, 25 °C) → Co (g, 25 °C)	$\Delta H_5 = 425.1 \pm 2.1$ [4]
Co (g, 25 °C) → Co^{3+} (g, 25 °C) + $3e^-$	$\Delta H_6 = 5641.1 \pm 5.8$ [5]
Co (g, 25 °C) → Co^{4+} (g, 25 °C) + $4e^-$	$\Delta H_7 = 10588 \pm 11$ [5]
O_2 (g, 25 °C) → 2O (g, 25 °C)	$\Delta H_8 = 498.458 \pm 0.004$ [6]
O (g, 25 °C) + $2e^-$ → O^{2-} (g, 25 °C)	$\Delta H_9 = 703$ [7]
For BLnC	
Ba (s, 25 °C) + Ln (s, 25 °C) + 2Co (s, 25 °C) + $(3-\delta/2)O_2$ (g, 25 °C) → $BaLnCo_2O_{6-\delta}$ (s, 25 °C)	$\Delta H_{10} = \Delta H_{f,el}$
Ba^{2+} (g, 25 °C) + Ln^{3+} (g, 25 °C) + $(1+2\delta)Co^{3+}$ (g, 25 °C) + $(1-2\delta)Co^{4+}$ (g, 25 °C) + $(6-\delta)O^{2-}$ (g, 25 °C) → $BaLnCo_2O_{6-\delta}$ (s, 25 °C)	U
$U = -\Delta H_1 - \Delta H_2 - \Delta H_3 - \Delta H_4 - 2\Delta H_5 - (1+2\delta)\Delta H_6 - (1-2\delta)\Delta H_7 - (3-\delta/2)\Delta H_8 - (6-\delta)\Delta H_9 + \Delta H_{10}$	
For BGLC	
xGd (s, 25 °C) + (1−x)La (s, 25 °C) → xGd (g, 25 °C) + (1−x)La (g, 25 °C)	ΔH_3
xGd (g, 25 °C) + (1−x)La (g, 25 °C) → xGd^{3+} (g, 25 °C) + $(1-x)La^{3+}$ (g, 25 °C) + $3e^-$	ΔH_4
Ba (s, 25 °C) + xGd (s, 25 °C) + (1−x)La (s, 25 °C)+ 2Co (s, 25 °C) + $(3-\delta/2)O_2$ (g, 25 °C) → $BaGd_xLa_{1-x}Co_2O_{6-\delta}$ (s, 25 °C)	$\Delta H_{10} = \Delta H_{f,el}$
Ba^{2+} (g, 25 °C) + xGd^{3+} (g, 25 °C) + $(1-x)La^{3+}$ (g, 25 °C) + $(1+2\delta)Co^{3+}$ (g, 25 °C) + $(1-2\delta)Co^{4+}$ (g, 25 °C) + $(6-\delta)O^{2-}$ (g, 25 °C) → $BaLnCo_2O_{6-\delta}$ (s, 25 °C)	U
$U = -\Delta H_1 - \Delta H_2 - \Delta H_3 - \Delta H_4 - 2\Delta H_5 - (1+2\delta)\Delta H_6 - (1-2\delta)\Delta H_7 - (3-\delta/2)\Delta H_8 - (6-\delta)\Delta H_9 + \Delta H_{10}$	

Table S3. Enthalpies of sublimation (ΔH_3) and ionization (ΔH_4) of Ln elements.

element	ΔH_3 (kJ mol^{-1})	ΔH_4 (kJ mol^{-1})
La	434.5 ± 3.0 [8]	3467.60 ± 0.08 [5]
Pr	356.6 ± 3.0 [8]	3639.9 ± 1.9 [5]
Nd	325.6 ± 2.0 [8]	3704.8 ± 4.3 [5]
Gd	406.9 ± 2.0 [8]	3740.3 ± 3.8 [5]

Table S4. BGLC37and BGLC82 as-prepared (AP) and after the stability treatment at 400 °C, 72 h in 1.5 bar of steam (ST).

sample	Space group	treatment	lattice parameters				χ^2	R_{wp}
			a (Å)	b (Å)	c (Å)	V (Å^3)		
BGLC37	Pmmm	AP	3.8941 (3)	7.8170 (5)	7.6876 (4)	234.01	1.31	2.72
BGLC37	Pmmm	ST	3.9039 (2)	7.8195 (5)	7.6534 (3)	233.63	1.37	5.06
BGLC82	Pmmm	AP	3.89054(5)	7.7963(1)	7.58061(8)	229.94	1.37	2.28
BGLC82	Pmmm	ST	3.8944 (4)	7.8001 (9)	7.5739 (6)	230.10	1.12	5.55

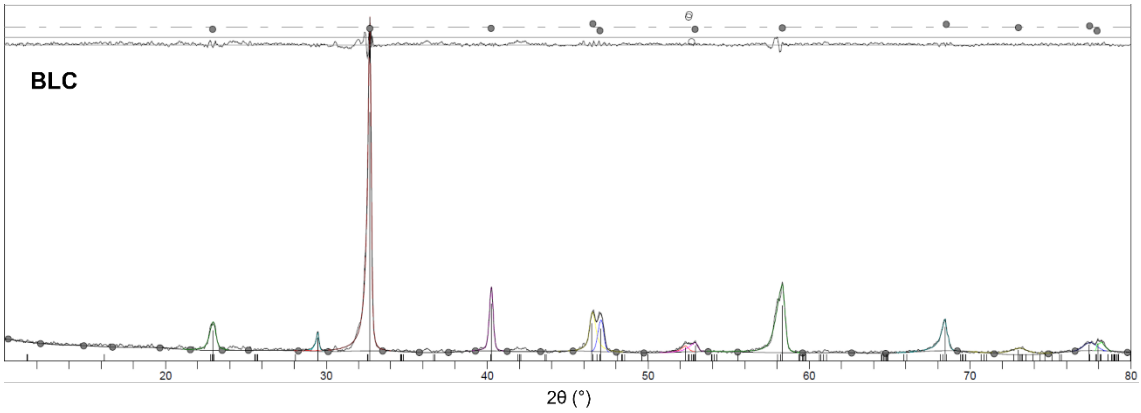

Figure S1. Profile fitting of the XRD pattern of BLC.

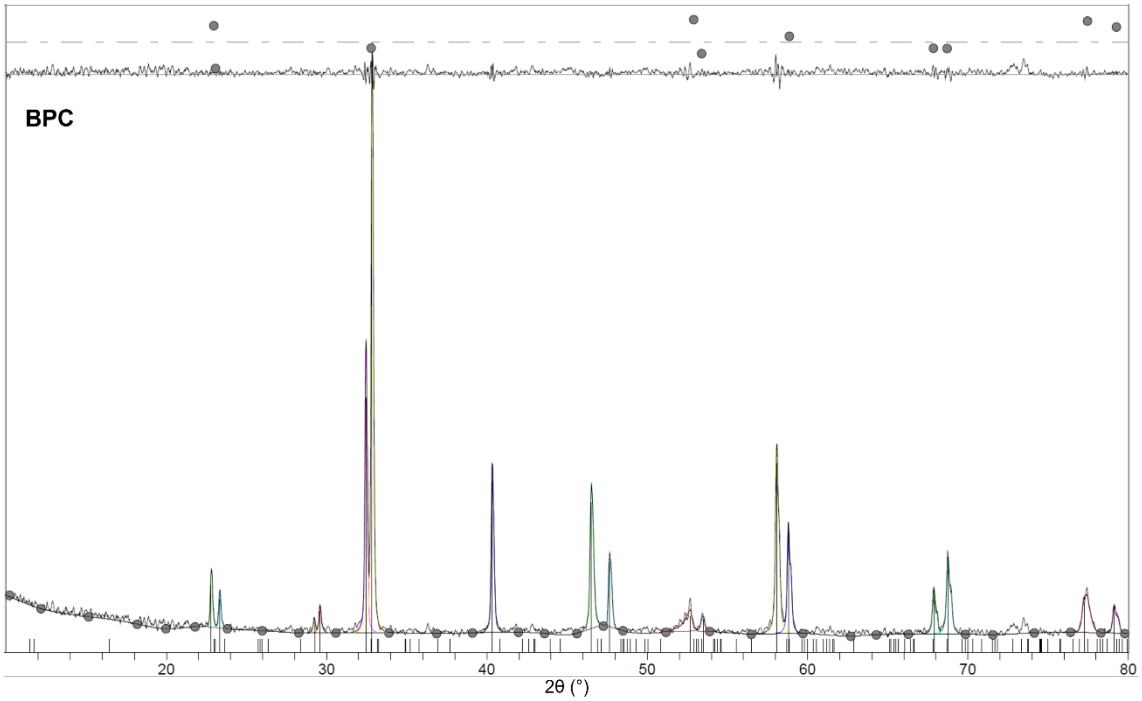

Figure S2. Profile fitting of the XRD pattern of BPC.

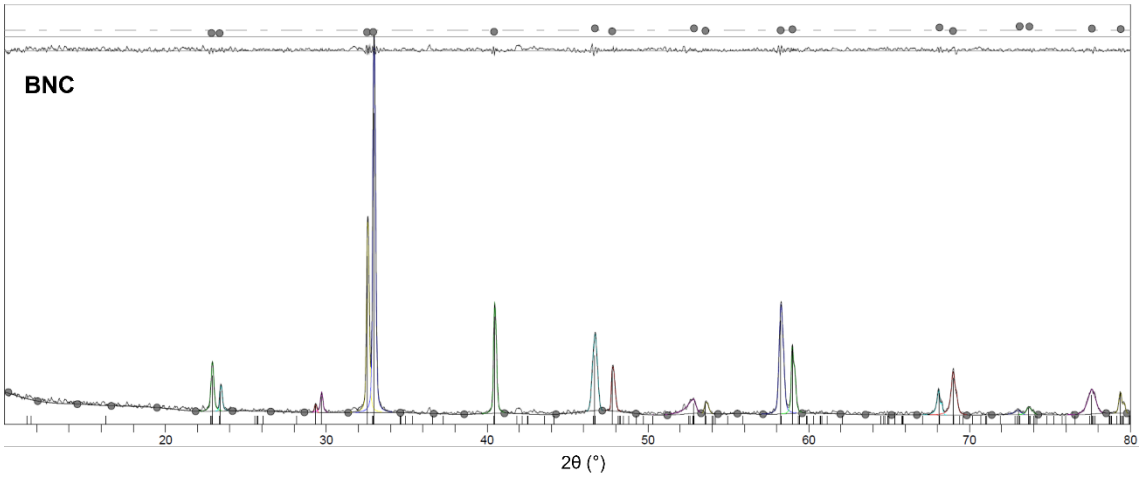

Figure S3. Profile fitting of the XRD pattern of BNC.

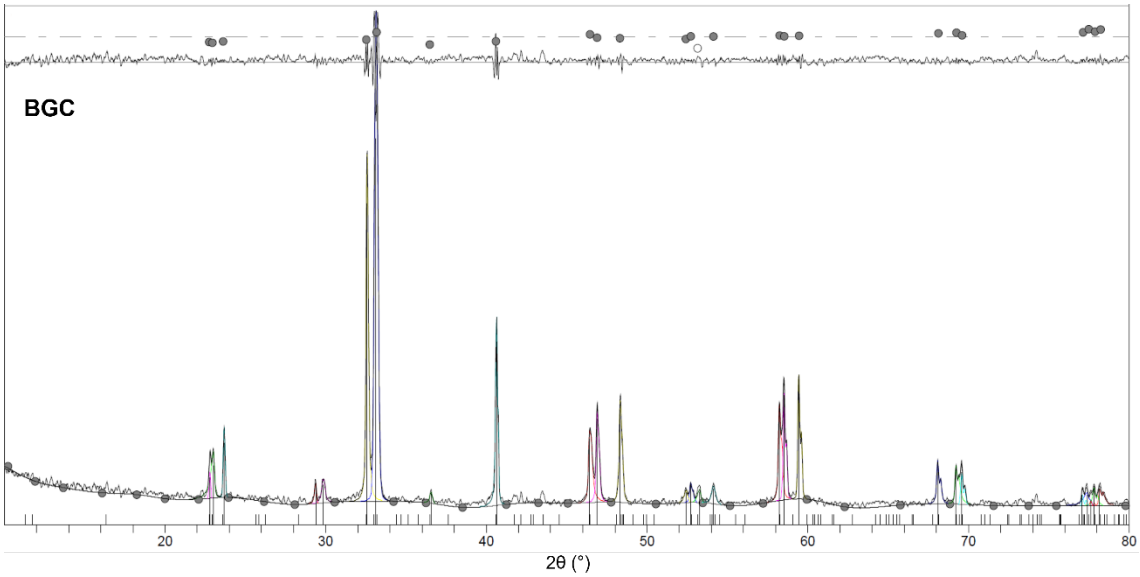

Figure S4. Profile fitting of the XRD pattern of BGC.

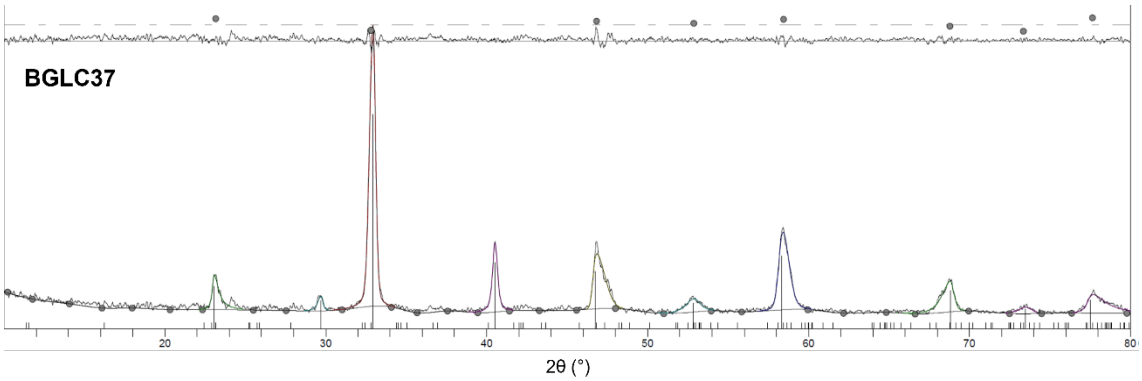

Figure S5. Profile fitting of the XRD pattern of BGLC37.

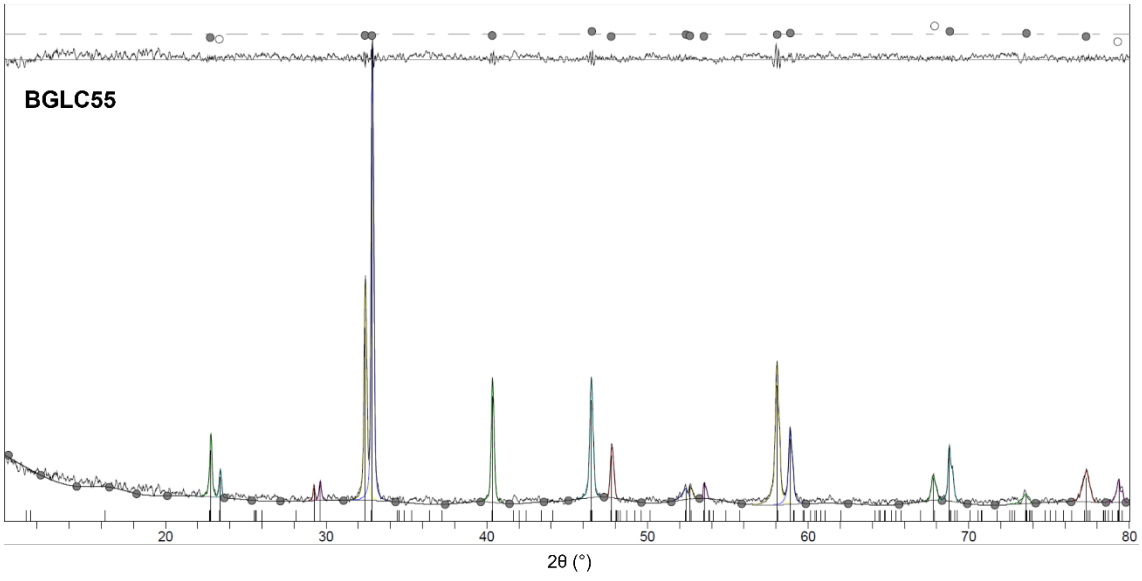

Figure S6. Profile fitting of the XRD pattern of BGLC55.

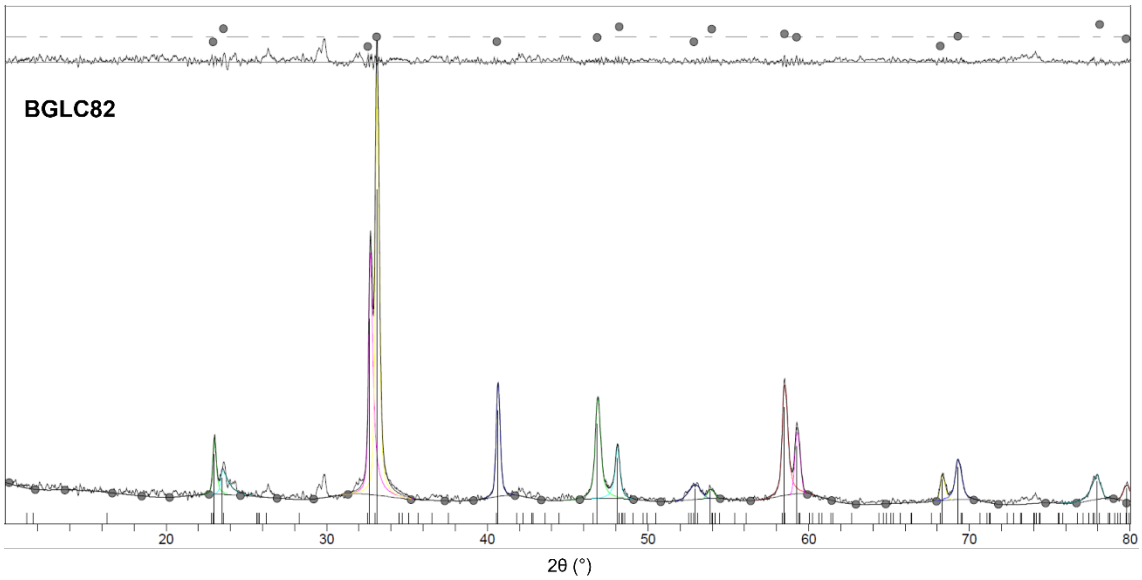

Figure S7. Profile fitting of the XRD pattern of BGLC82.

References:

(1) Anna, S.; Adel, M.; Stéphanie, S.; Nicolas, C.; Nicolas, D.; Alexandra, N. Thermodynamics and stability of rhabdophanes, hydrated rare earth phosphates $REPO_4 \cdot n\ H_2O$. *Front. Chem.* **2018**, *6*, 604.

(2) Ushakov, S. V.; Helean, K. B.; Navrotsky, A.; Boatner, L. A. Thermochemistry of rare-earth orthophosphates. *J. Mater. Res.* **2001**, *16*, 2623–2633.

(3) Konings, R. J. M.; Beneš, O.; Kovács, A.; Manara, D.; Sedmidubský, D.; Gorokhov, L.; Iorish, V. S.; Yungman, V.; Shenyavskaya, E.; Osina, E. The thermodynamic properties of the f-elements and their compounds. Part 2. The lanthanide and actinide oxides. *J. Phys. Chem. Ref. Data* **2014**, *43*, 013101.

(4) Chase, M. W., Jr. *NIST-JANAF Thermochemical Tables*. 4th ed.; J. Phys. Chem. Ref. Data, Monograph, 1998; Vol. 9, pp 1– 1951.

(5) Kramida, A.; Ralchenko, Yu.; Reader, J.; NIST ASD Team (2021). *NIST Atomic Spectra Database* (ver. 5.9), https://physics.nist.gov/asd (accessed 2022-06-01).

(6) Rumble, J. R. *CRC Handbook of Chemistry and Physics*, 101st ed.; CRC Press/Taylor & Francis, 2020.

(7) Atkins, P.; de Paula, J.; Keeler, J. *Atkins' Physical Chemistry*, 11th ed.; Oxford University Press, 2018.

(8) Konings, R. J. M.; Beneš, O. The thermodynamic properties of the f-elements and their compounds. I. The lanthanide and actinide metals. *J. Phys. Chem. Ref. Data* **2010**, *39*, 043102.